VIP Infrared Spectroscopy

DOI: 10.1002/anie.201108937

Infrared Spectrum and Structure of the Adamantane Cation: Direct Evidence for Jahn–Teller Distortion**

*Alexander Patzer, Markus Schütz, Thomas Möller, and Otto Dopfer**

Adamantane ($C_{10}H_{16}$, Figure 1) is the parent molecule of diamondoids, a recently established important class of hydrocarbon molecules.[1,2] Diamondoids are rigid and stress-free cycloalkanes, which can be considered as nanometer-sized

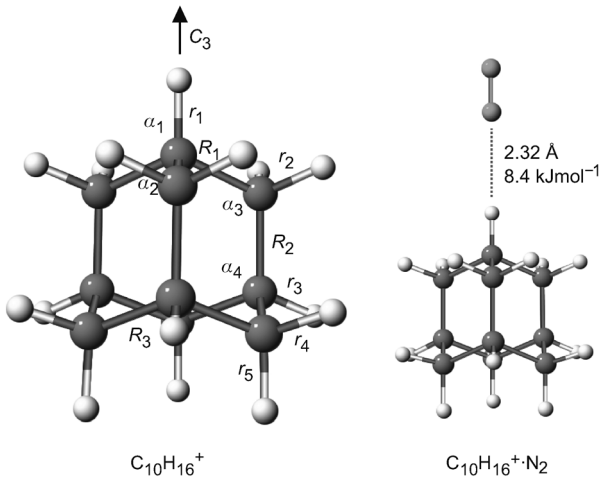

Figure 1. Structures of $C_{10}H_{16}^+$ and the most stable $C_{10}H_{16}^+ \cdot N_2$ dimer calculated at the B3LYP/cc-pVDZ level. Relevant structural parameters are listed in Table T1 in the Supporting Information.

H-terminated diamond-like alkanes with well-defined structures. The unique and largely variable properties of diamondoids and their derivatives make them promising building blocks for new nanomaterials with tailored mechanical, electronic, optical, and chemical properties, with applications in materials and polymer sciences, molecular electronics, biomedical sciences, and chemical synthesis.[2–4] Moreover, the high stability of nanodiamondoids suggests their presence in interstellar environments.[5] Here, we report the IR spectrum of the adamantane radical cation, which provides the first spectroscopic characterization of the geometric and electronic structure of this prototypical carbocation.

Quantum chemical calculations, IR and Raman spectroscopy,[6] and electron diffraction[7] show that $C_{10}H_{16}$ has a highly symmetric structure with tetrahedral symmetry. Its 76 electrons are distributed in molecular orbitals classified in the T_d point group by $\Gamma_e = 5a_1 + 3e + 2t_1 + 7t_2$, leading to a $^1A_1$ ground electronic state. Removal of one electron from the fully occupied $(7t_2)^6$ HOMO generates a $^2T_2$ ground electronic state for $C_{10}H_{16}^+$ in the T_d point group. This state is however subject to Jahn–Teller (J-T) distortion, leading to a structure with C_{3v} symmetry (Figure 1). As a consequence, the $(7t_2)^5$ configuration of the HOMO splits into $(12e)^4(12a_1)^1$, which generates a $^2A_1$ ground electronic state of $C_{10}H_{16}^+$ (Figure 2).

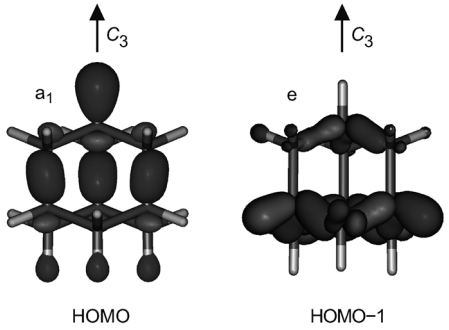

Figure 2. HOMO ($12a_1$) and HOMO-1 ($12e$) orbitals of $C_{10}H_{16}^+$ in C_{3v} symmetry arising from the splitting of the triply degenerate $7t_2$ orbital upon Jahn–Teller distortion.

This view is not only supported by calculations[3,8] but also indirectly inferred from Rydberg[9] and low-resolution photoelectron spectra of $C_{10}H_{16}$.[9a,10] The photoelectron and Penning ionization spectra of the ground electronic state of $C_{10}H_{16}^+$ are broad, because the $7t_2$ orbital is strongly σ_{cc}-bonding (Figure 2) and removal of an electron induces J-T distortion, leading to the congested unresolved ionization spectra.[10] Despite considerable efforts, IR and electronic spectra of (isolated) $C_{10}H_{16}^+$ at the level of vibrational or higher resolution are lacking in the gas and condensed phase, because of the challenge involved in the production of sufficient concentrations required for spectroscopic interrogation of this highly reactive and elusive hydrocarbon ion. However, such spectra are required to confirm and directly measure the extent of the predicted J-T distortion in this fundamental carbocation. In addition, laboratory spectra of $C_{10}H_{16}^+$ are requested from the astrochemical community for direct comparison with astronomical spectra, because diamond-like material has been proposed to carry more than 5% of cosmic carbon and 40% or tertiary carbon in interstellar environments.[5]

[*] Dipl.-Phys. A. Patzer, B. Sc. M. Schütz, Prof. Dr. T. Möller, Prof. Dr. O. Dopfer
Institut für Optik und Atomare Physik
Technische Universität Berlin
Hardenbergstr. 36, 10623 Berlin (Germany)
E-mail: dopfer@physik.tu-berlin.de

[**] This study was supported by the Deutsche Forschungsgemeinschaft within the research unit FOR 1282 (grant numbers DO 729/5 and MO 719/10).

Supporting information for this article is available on the WWW under http://dx.doi.org/10.1002/anie.201108937.

Here we report the IR spectrum of isolated $C_{10}H_{16}^+$ in the CH stretching range (σ_{CH}) obtained through He-tagging IR photodissociation (IRPD). This sensitive IRPD approach was previously used to elucidate the structure of related fundamental hydrocarbon ions, such as $C_2H_5^+$,[11] $C_3H_3^+$,[12] $C(OH)_3^+$,[13] $C_6H_5^+$,[14] and $C_6H_7^+$.[15] Weakly bound He or N_2 ligands are attached to $C_{10}H_{16}^+$ to facilitate resonant single-photon fragmentation, as shown in Figure 3 for $C_{10}H_{16}^+$·He_2

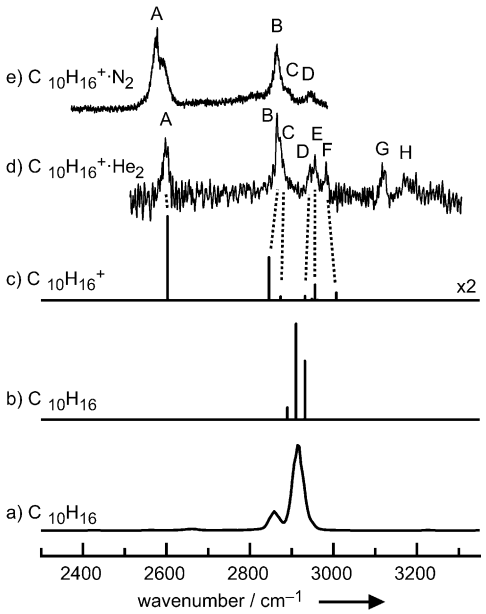

Figure 3. The experimental IRPD spectra of e) $C_{10}H_{16}^+$·N_2 and d) $C_{10}H_{16}^+$·He_2 are compared to the linear stick IR absorption spectra of c) $C_{10}H_{16}^+$ and b) $C_{10}H_{16}$ in their $^2A_1$ and $^1A_1$ ground electronic states, respectively, calculated at the B3LYP/cc-pVDZ level. For comparison, the experimental IR absorption spectrum of $C_{10}H_{16}$ taken from the NIST database is shown as well in (a).[21] The positions and assignments of the transitions are listed in Table 1.

and $C_{10}H_{16}^+$·N_2. Due to the very small $C_{10}H_{16}^+$·He binding energy ($D_0 < 1$ kJ mol^{-1}),[16] the influence of He atoms on the $C_{10}H_{16}^+$ spectrum is very weak and considered negligible.[16,17] This assumption is supported by IRPD spectra of $C_{10}H_{16}^+$·He_n with $n = 1$–3, which are identical in appearance at the current spectral resolution (around 5 cm^{-1}). Thus, the IRPD spectrum of $C_{10}H_{16}^+$·He_2 in Figure 3d provides a very good approximation of the IR absorption spectrum of bare $C_{10}H_{16}^+$.[18] This spectrum shows at least eight transitions in the 2500–3300 cm^{-1} range (denoted A–H), which occur in all $C_{10}H_{16}^+$·He_n spectra at the same positions (to within 1 cm^{-1}) and are mostly assigned to σ_{CH} fundamentals of the J-T-distorted $C_{10}H_{16}^+$.

B3LYP/cc-pVDZ calculations elucidate the energetic, structural, electronic, and vibrational properties of $C_{10}H_{16}$ and its cation.[19,20] The two distinguishable CH equilibrium bond lengths of the four CH and six CH_2 units in neutral $C_{10}H_{16}$ ($r_1 = 1.1037$ Å, $r_2 = 1.1043$ Å) are consistent with the experimental values derived from electron diffraction ($r_1 \approx r_2 = 1.112 \pm 0.004$ Å).[7] The 16 CH local modes give rise to 7 σ_{CH} fundamentals (ν_i, $i = 1$–7), with predicted wavenumbers in the 2880–2940 cm^{-1} interval. Only three of them are IR-active, and their predicted wavenumbers occur in the narrow 2890–2940 cm^{-1} range, consistent with the experimental spectrum reproduced in Figure 3d.[21] All bond angles are close to a tetrahedral configuration ($109 \pm 1°$),[7] except for the CH_2 scissoring angle (106.8°). The J-T-distorted $^2A_1$ ground electronic state of $C_{10}H_{16}^+$ is generated by removal of one electron from the HOMO a_1 orbital, and the calculated ionization energy of 8.77 eV is consistent[5e,8c] with available experimental values (9.1–9.4 eV).[10,21,22] This orbital has a strong bonding character at a single CH bond (r_1) and three CC bonds (R_2), all of which are nearly parallel to the rotational C_3 symmetry axis (Figure 2). Hence, the major structural changes upon ionization involve drastic elongations of the corresponding CH and CC bonds, $\Delta r_1 = +0.030$ Å and $\Delta R_2 = +0.070$ Å, and a minor elongation of $\Delta r_5 = +0.005$ Å. In contrast, all other CH and CC bonds show less pronounced bond contractions in the range of 0.002–0.026 Å. As a further consequence of the J-T distortion of the regular $C_{10}H_{16}$ cage, many bond angles in the cation also deviate substantially from the tetrahedral configuration.[8] The energy gain upon $T_d \rightarrow C_{3v}$ symmetry relaxation arising from J-T distortion is calculated as 14.7 kJ mol^{-1} (6.6 kJ mol^{-1} including zero-point energy corrections).[23] Comparison of the natural bond orbital charge distribution of $C_{10}H_{16}$ and $C_{10}H_{16}^+$ detailed in Figure S1 in the Supporting Information is consistent with removal of one electron from the bonding HOMO a_1 orbital, which contributes mainly to the three CC σ bonds connecting the top and bottom parts of the adamantane cage (i.e., the C_4H_7 and C_6H_9 units). In addition, the charges of all H atoms increase by $\Delta q_H = 0.02$–0.07 e upon ionization ($q_H = 0.26$–0.29 e), with the notable exception of the most acidic proton on the C_3 axis, the charge of which increases by $\Delta q_H = 0.15$ e ($q_H = 0.38$ e). Due to its high positive partial charge, this H atom is the most favorable attractor for ligands L in C–H···L hydrogen bonding in $C_{10}H_{16}^+$·L. For the same reason, it is also the preferential H atom eliminated in dissociation of $C_{10}H_{16}^+$ into the most stable 1-$C_{10}H_{15}^+$ isomer of the adamantyl cation.[3,5e,24] Loss of this proton is also invoked in proton transfer reactions of $C_{10}H_{16}^+$ in solution.[3,8a]

The structural and electronic changes upon ionization of $C_{10}H_{16}$ are directly reflected by its vibrational spectrum, and the implications for the CH stretching range are visualized in Figure 3. Symmetry reduction from T_d to C_{3v} induces splittings of the degenerate σ_{CH} modes with $t_{1/2}$ symmetry into $a_{2/1} + e$ (Table 1). The σ_{CH} modes transform as $\Gamma_{CH} = 2a_1 + e + t_1 + 3t_2$ in T_d ($C_{10}H_{16}$) and as $\Gamma_{CH} = 5a_1 + a_2 + 5e$ in C_{3v} ($C_{10}H_{16}^+$). Moreover, the larger spread in CH bond lengths in the cation compared to the neutral molecule ($r_{1-5} = 1.0992$–1.1333 vs. 1.1037–1.1043 Å) produces a larger spread in the corresponding σ_{CH} wavenumbers ($\nu_{1-7} = 2602$–3007 vs. 2886–2931 cm^{-1}). A decomposition of the CH normal modes into the CH local modes is given in Table T2 in the Supporting Information, which shows a clear correlation between the CH bond lengths r_i and the associated σ_{CH} wavenumbers. The IR selection rules are such that only t_2 modes are IR-active in T_d, whereas a_1 and e modes become IR-allowed in C_{3v}. Hence, the number of IR-active σ_{CH} modes increases from three to ten upon ionization, leading to a much richer IR spectrum for the

Table 1: CH stretching wavenumbers (σ_{CH} in cm^{-1}) of $C_{10}H_{16}$ and $C_{10}H_{16}^+$ calculated at the B3LYP/cc-pVDZ level compared to experimental values of $C_{10}H_{16}$, $C_{10}H_{16}^+\cdot He_2$, and $C_{10}H_{16}^+\cdot N_2$ (Figure 3).

Mode[a]	$C_{10}H_{16}$ (T_d, $^1A_1$)[b]	$C_{10}H_{16}$ exp[c]	Mode[a]	$C_{10}H_{16}^+$ (C_{3v}, $^2A_1$)[b]	$C_{10}H_{16}^+\cdot He_2$ exp	$C_{10}H_{16}^+\cdot N_2$ exp	$C_{10}H_{16}^+\cdot N_2$ (C_{3v}, $^2A_1$)[b]
$\nu_1(t_2)$	2931 (276)	2940	$\nu_1(e)$	3007 (19)	2981 (F)		3005 (20)
$\nu_2(t_1)$	2927 (0)		$\nu_2(a_2)$	3002 (0)			3001 (0)
$\nu_3(a_1)$	2922 (0)	2950	$\nu_3(a_1)$	2962 (1)			2961 (1)
$\nu_4(t_2)$	2910 (450)	2910	$\nu_2(e)$	2955 (36)	2954 (E)		2955 (43)
$\nu_5(e)$	2891 (0)	2900	$\nu_1(a_1)$	2949 (2)			2949 (2)
$\nu_6(t_2)$	2890 (57)	2850	$\nu_5(e)$	2948 (0.5)			2948 (0.07)
$\nu_7(a_1)$	2886 (0)	2913	$\nu_4(a_1)$	2941 (0.05)			2941 (0.3)
			$\nu_4(e)$	2932 (10)	2941 (D)	2945 (D)	2932 (9)
			$\nu_6(a_1)$	2873 (9)	2883 (C)	2889 (C)	2879 (5)
			$\nu_6(e)$	2846 (101)	2868 (B)	2864 (B)	2854 (78)
			$\nu_7(a_1)$	2602 (197)	2600 (A)	2575 (A)	2553 (827)
			[d]		3120 (G)		
			[d]		3177 (H)		

[a] See Table T2 in the Supporting Information for a description of the normal modes. [b] IR intensities I_{CH} in km mol^{-1} are listed in parentheses. Harmonic wavenumbers are scaled by 0.96. [c] Ref. [6c]. Some assignments may not be reliable because of inconsistent literature reports.[6] [d] See ref. [25] for tentative assignments.

$C_{10}H_{16}^+$ cation. Six out of the ten active σ_{CH} fundamentals of $C_{10}H_{16}^+$ have predicted IR oscillator strengths with $I_{CH} > 2$ km mol^{-1} and are thus visible in the computed spectrum in Figure 3c. In addition to vibrational splittings, ionization has a drastic impact on the σ_{CH} wavenumbers and the composition of the normal modes in the basis of the CH local modes. Most significantly, $C_{10}H_{16}^+$ shows an intense and isolated σ_{CH} local mode with a very unusual low wavenumber of $\nu_7(a_1)$ around 2600 cm^{-1} associated with the single weak CH bond (r_1). This unique spectral feature is largely separated (by around 250 cm^{-1}) from the other σ_{CH} modes (around 2850–3000 cm^{-1}) and thus constitutes the characteristic spectroscopic signature of the J-T-distorted $C_{10}H_{16}^+$ cation in this spectral range.

The IR spectrum calculated for $C_{10}H_{16}^+$ in Figure 3c compares favorably with the IRPD spectrum measured for $C_{10}H_{16}^+\cdot He_2$ in Figure 3d with respect to both the wavenumbers and relative IR intensities of the σ_{CH} fundamentals. The transitions A–F can readily be assigned to all six σ_{CH} modes with $I_{CH} > 2$ km mol^{-1}, indicating the high sensitivity of the experimental approach. The maximal and average deviations of less than 26 and 12 cm^{-1} from the predicted wavenumbers are compatible with the resolution of the spectroscopic approach (around 5 cm^{-1}). Thus, the IRPD spectrum of $C_{10}H_{16}^+\cdot He_2$ provides for the first time compelling spectroscopic evidence of the J-T distortion in the $^2A_1$ ground state of $C_{10}H_{16}^+$. Clearly, the IR spectrum predicted for a $^2T_2$ ground state of the cation with T_d symmetry is not compatible with the experiment (see Figure S2 in the Supporting Information). Bands G and H at 3120 and 3177 cm^{-1} in the IRPD spectrum of $C_{10}H_{16}^+\cdot He_2$ cannot arise from σ_{CH} fundamentals of $C_{10}H_{16}^+$ and are currently assigned to overtone and/or combination bands.[25]

The IRPD spectrum of $C_{10}H_{16}^+\cdot N_2$ in Figure 3e provides a sensitive probe of the hydrogen bonding interaction of the acidic CH proton in the J-T-distorted ground state of $C_{10}H_{16}^+$. Such experimental data yield information of H-bonded $C_{10}H_{16}^+\cdot L$ complexes, which are invoked as reaction intermediates in functionalization reactions of adamantane.[3,26] B3LYP calculations show that the H-bonded $C_{10}H_{16}^+\cdot N_2$ dimer with C_{3v} symmetry displayed in Figure 1 is by far the most stable isomer of the intermolecular potential. The anisotropy of the polarizability and the negative quadrupole moment favor a linear over a T-shaped approach of the N_2 ligand toward the positive charge.[12a,16b,27] The intermolecular bond is characterized by $R = 2.32$ Å and a binding energy of $D_0 = 8.4$ kJ mol^{-1} (699 cm^{-1}). Thus, while the interaction of the inert He atom with $C_{10}H_{16}^+$ is negligible ($D_0 < 1$ kJ mol^{-1}), the N_2 ligand has appreciable impact on the geometric and IR spectral properties of the core ion (see Table 1, Table T1, and Figure S3 in the Supporting Information). Most significantly, the CH proton donor bond is elongated by $\Delta r_1 = 0.005$ Å, which results in a noticeable red shift of the corresponding σ_{CH} wavenumber of this isolated mode, $\Delta\nu_7(a_1) = -50$ cm^{-1}, and a fourfold increase in its IR intensity. All other CH bond lengths and σ_{CH} wavenumbers are much less affected upon formation of the H bond ($|\Delta r| < 0.0006$ Å, $|\Delta\sigma_{CH}| < 8$ cm^{-1}). Comparison of the IRPD spectra of $C_{10}H_{16}^+\cdot N_2$ and $C_{10}H_{16}^+\cdot He_2$ in Figure 3 confirms these theoretical predictions. Both spectra are very similar in appearance (bands B–D have the same wavenumbers to within 6 cm^{-1}), with the notable exception of the red-shifted and enhanced transition A assigned to $\nu_7(a_1)$. The measured shift of $\Delta\nu_7(a_1) = -25$ cm^{-1} for $C_{10}H_{16}^+\cdot N_2$ is somewhat smaller than the predicted value, which may indicate that the B3LYP/cc-pVDZ level slightly overestimates the strength of the intermolecular H bond.[28] Significantly, the IRPD spectrum of H-bonded $C_{10}H_{16}^+\cdot N_2$ confirms the enhanced acidity of the CH bond r_1 of $C_{10}H_{16}^+$ and thus the J-T-distorted geometry of $C_{10}H_{16}^+$ in its $^2A_1$ state.

In conclusion, He-tagging IRPD spectroscopy provides the first spectroscopic and structural characterization of $C_{10}H_{16}^+$ in the gas phase. The analysis of the σ_{CH} wavenumbers provides details of the CH bond properties in this fundamental alkane cation. Significantly, the IRPD spectrum provides the first compelling spectroscopic evidence for a J-T distortion of $C_{10}H_{16}^+$ leading to a $^2A_1$ ground electronic state with C_{3v} symmetry. The unusually low σ_{CH} wavenumber of 2600 cm^{-1} for $\nu_7(a_1)$ is a unique characteristic fingerprint of

the $C_{10}H_{16}^+$ cation and may readily be used for its identification in hydrocarbon plasmas, including the interstellar medium. Future experiments aim at the measurement of IR and optical spectra of $C_{10}H_{16}^+$, higher diamondoids, their derivatives, and their clusters to probe the effects of functionalization, solvation, and adsorption on the geometric and electronic structure of these fundamental carbocations.

Experimental Section

IRPD spectra of $C_{10}H_{16}^+\cdot L_n$ with L = He and N_2 were recorded in a tandem quadrupole mass spectrometer (QMS1/2).[29] Cold $C_{10}H_{16}^+\cdot L_n$ clusters with a rotational temperature of less than 50 K were generated in a pulsed supersonic plasma beam expansion of $C_{10}H_{16}$ ($T = 150\,°C$) seeded in 36 bar of He or 5 bar of N_2 carrier gas. Weakly bound $C_{10}H_{16}^+\cdot L_n$ ions were produced by electron ionization of $C_{10}H_{16}$ and subsequent three-body aggregation. The $C_{10}H_{16}^+\cdot L_n$ clusters were mass-selected by QMS1 and irradiated in an octopole ion trap with a tunable IR laser pulse (ν_{IR}) generated by a pulsed OPO laser with a bandwidth of $1\,cm^{-1}$. Resonant vibrational excitation of $C_{10}H_{16}^+\cdot L_n$ induced the rupture of the weak intermolecular bonds [Eq. (1)]:

$$C_{10}H_{16}^+ \cdot L_n + h\nu_{IR} \rightarrow C_{10}H_{16}^+ + n\,L \quad (1)$$

$C_{10}H_{16}^+$ fragment ions were selected by QMS2 and monitored as a function of ν_{IR} to obtain IRPD spectra of $C_{10}H_{16}^+\cdot L_n$. The resolution of the spectroscopic approach is limited by unresolved rotational substructure, leading to widths of around 10 and around $20\,cm^{-1}$ of the vibrational transitions for L = He and N_2, respectively.[30] Quantum chemical calculations were carried out at the B3LYP/cc-pVDZ level.[19,20] Binding energies were corrected for zero-point vibrational energies. Harmonic vibrational wavenumbers were scaled by 0.96.[20]

Received: December 19, 2011
Published online: January 27, 2012

Keywords: adamantane · carbocations · IR spectroscopy · Jahn–Teller effect · structure elucidation

[1] a) P. v. R. Schleyer, *J. Am. Chem. Soc.* **1957**, *79*, 3292; b) R. C. Fort, P. v. R. Schleyer, *Chem. Rev.* **1964**, *64*, 277.

[2] a) J. E. Dahl, S. G. Liu, R. M. K. Carlson, *Science* **2003**, *299*, 96; b) J. E. P. Dahl, J. M. Moldowan, Z. B. Wei, P. A. Lipton, P. Denisevich, R. Gat, S. G. Liu, P. R. Schreiner, R. M. K. Carlson, *Angew. Chem.* **2010**, *122*, 10077; *Angew. Chem. Int. Ed.* **2010**, *49*, 9881.

[3] A. A. Fokin, P. R. Schreiner, *Chem. Rev.* **2002**, *102*, 1551.

[4] a) J. Y. Raty, G. Galli, *Nat. Mater.* **2003**, *2*, 792; b) P. R. Schreiner, N. A. Fokina, B. A. Tkachenko, H. Hausmann, M. Serafin, J. E. P. Dahl, S. G. Liu, R. M. K. Carlson, A. A. Fokin, *J. Org. Chem.* **2006**, *71*, 6709; c) H. Schwertfeger, A. A. Fokin, P. R. Schreiner, *Angew. Chem.* **2008**, *120*, 1038; *Angew. Chem. Int. Ed.* **2008**, *47*, 1022; d) Y. Y. Wang, E. Kioupakis, X. H. Lu, D. Wegner, R. Yamachika, J. E. Dahl, R. M. K. Carlson, S. G. Louie, M. F. Crommie, *Nat. Mater.* **2008**, *7*, 38; e) L. Landt, K. Klunder, J. E. Dahl, R. M. K. Carlson, T. Möller, C. Bostedt, *Phys. Rev. Lett.* **2009**, *103*, 4; f) H. Schwertfeger, P. R. Schreiner, *Chem. Unserer Zeit* **2010**, *44*, 248; g) P. R. Schreiner, L. V. Chernish, P. A. Gunchenko, E. Y. Tikhonchuk, H. Hausmann, M. Serafin, S. Schlecht, J. E. P. Dahl, R. M. K. Carlson, A. A. Fokin, *Nature* **2011**, *477*, 308; h) W. L. Yang, J. D. Fabbri, T. M. Willey, J. R. I. Lee, J. E. Dahl, R. M. K. Carlson, P. R. Schreiner, A. A. Fokin, B. A. Tkachenko, N. A. Fokina, W. Meevasana, N. Mannella, K. Tanaka, X. J. Zhou, T. van Buuren, M. A. Kelly, Z. Hussain, N. A. Melosh, Z. X. Shen, *Science* **2007**, *316*, 1460.

[5] a) D. F. Blake, F. Freund, K. F. M. Krishnan, C. J. Echer, R. Shipp, T. E. Bunch, A. G. Tielens, R. J. Lipari, C. J. D. Hetherington, S. Chang, *Nature* **1988**, *332*, 611; b) R. S. Lewis, E. Anders, B. T. Draine, *Nature* **1989**, *339*, 117; c) L. J. Allamandola, S. A. Sandford, A. Tielens, T. M. Herbst, *Science* **1993**, *260*, 64; d) O. Pirali, M. Vervloet, J. E. Dahl, R. M. K. Carlson, A. Tielens, J. Oomens, *Astrophys. J.* **2007**, *661*, 919; e) M. Steglich, F. Huisken, J. E. Dahl, R. M. K. Carlson, T. Henning, *Astrophys. J.* **2011**, *729*, 10; f) C. W. Bauschlicher, Jr., Y. F. Liu, A. Ricca, A. L. Mattioda, L. J. Allamandola, *Astrophys. J.* **2007**, *671*, 458.

[6] a) R. T. Bailey, *Spectrochim. Acta Part A* **1971**, *27*, 1447; b) T. E. Jenkins, J. Lewis, *Spectrochim. Acta Part A* **1980**, *36*, 259; c) L. Bistricic, G. Baranovic, K. Mlinaricmajerski, *Spectrochim. Acta Part A* **1995**, *51*, 1643; d) J. O. Jensen, *Spectrochim. Acta Part A* **2004**, *60*, 1895.

[7] I. Hargittai, K. Hedberg, *J. Chem. Soc. D* **1971**, 1499.

[8] a) A. A. Fokin, P. R. Schreiner, P. A. Gunchenko, S. A. Peleshanko, T. E. Shubina, S. D. Isaev, P. V. Tarasenko, N. I. Kulik, H. M. Schiebel, A. G. Yurchenko, *J. Am. Chem. Soc.* **2000**, *122*, 7317; b) G. Yan, N. R. Brinkmann, H. F. Schaefer, *J. Phys. Chem. A* **2003**, *107*, 9479; c) A. A. Novikovskii, P. A. Gunchenko, P. G. Prikhodchenko, Y. A. Serguchev, P. R. Schreiner, A. A. Fokin, *Russ. J. Org. Chem.* **2011**, *47*, 1293.

[9] a) J. W. Raymonda, *J. Chem. Phys.* **1972**, *56*, 3912; b) B. A. Heath, N. A. Kuebler, M. B. Robin, *J. Chem. Phys.* **1979**, *70*, 3362; c) Q. Y. Shang, E. R. Bernstein, *J. Chem. Phys.* **1994**, *100*, 8625.

[10] a) S. D. Worley, G. D. Mateescu, C. McFarlan, R. C. Fort, C. F. Sheley, *J. Am. Chem. Soc.* **1973**, *95*, 7580; b) W. Schmidt, *Tetrahedron* **1973**, *29*, 2129; c) S. X. Tian, N. Kishimoto, K. Ohno, *J. Phys. Chem. A* **2002**, *106*, 6541.

[11] a) H. S. Andrei, N. Solca, O. Dopfer, *Angew. Chem.* **2008**, *120*, 401; *Angew. Chem. Int. Ed.* **2008**, *47*, 395; b) A. M. Ricks, G. E. Douberly, P. v. R. Schleyer, M. A. Duncan, *Chem. Phys. Lett.* **2009**, *480*, 17.

[12] a) O. Dopfer, D. Roth, J. P. Maier, *J. Am. Chem. Soc.* **2002**, *124*, 494; b) M. Ricks, G. E. Douberly, P. v. R. Schleyer, M. A. Duncan, *J. Chem. Phys.* **2010**, *132*, 051101; c) P. Botschwina, R. Oswald, O. Dopfer, *Phys. Chem. Chem. Phys.* **2011**, *13*, 14163.

[13] H. S. Andrei, S. A. Nizkorodov, O. Dopfer, *Angew. Chem.* **2007**, *119*, 4838; *Angew. Chem. Int. Ed.* **2007**, *46*, 4754.

[14] A. Patzer, S. Chakraborty, N. Solca, O. Dopfer, *Angew. Chem.* **2010**, *122*, 10343; *Angew. Chem. Int. Ed.* **2010**, *49*, 10145.

[15] a) N. Solcà, O. Dopfer, *Angew. Chem.* **2002**, *114*, 3781; *Angew. Chem. Int. Ed.* **2002**, *41*, 3628; b) N. Solcà, O. Dopfer, *Chem. Eur. J.* **2003**, *9*, 3154; c) G. E. Douberly, M. Ricks, G. E. Douberly, P. v. R. Schleyer, M. A. Duncan, *J. Phys. Chem. A* **2008**, *112*, 4869.

[16] a) The $C_{10}H_{16}^+\cdot N_2$ interaction energy is calculated as around $10\,kJ\,mol^{-1}$. As the binding energy of He to cations is typically at least 10 times weaker than for N_2,[16b] the $C_{10}H_{16}^+\cdot He$ interaction energy is estimated to be $< 1\,kJ\,mol^{-1}$; b) R. V. Olkhov, O. Dopfer, *Chem. Phys. Lett.* **1999**, *314*, 215.

[17] a) O. Dopfer, R. V. Olkhov, J. P. Maier, *J. Chem. Phys.* **1999**, *111*, 10754; b) N. Solcà, O. Dopfer, *J. Phys. Chem. A* **2001**, *105*, 5637; c) O. Dopfer, M. Meuwly, S. A. Nizkorodov, E. J. Bieske, J. P. Maier, *Chem. Phys. Lett.* **1996**, *260*, 545.

[18] The IRPD spectrum of $C_{10}H_{16}^+\cdot He_n$ with $n = 2$ is selected because it shows the best signal-to-noise ratio.

[19] M. J. Frisch et al., Gaussian09, Revision A.02, Gaussian Inc., Wallingford CT, **2009** (see the Supporting Information).

[20] The scaling factor of 0.96 optimizes the agreement between experimental and theoretical σ_{CH} wavenumbers of $C_{10}H_{16}$. B3LYP calculations with larger basis sets result in similar results as for the cc-pVDZ basis (see Figure S4 in the Supporting

Information). Spin contamination at the B3LYP level is negligible ($S^2-0.75 < 0.002$ before annihilation). MP2 calculations are not suitable for degenerate electronic states affected by Jahn–Teller distortion (like in $C_{10}H_{16}^+$) and yield unrealistic IR spectra.

[21] P. J. Linstrom, W. G. Mallard, *NIST Chemistry WebBook*, NIST Standards and Technology, Gaithersburg MD, 20899 (http://webbook.nist.gov), **2011**.

[22] K. Lenzke, L. Landt, M. Hoener, H. Thomas, J. E. Dahl, S. G. Liu, R. M. K. Carlson, T. Möller, C. Bostedt, *J. Chem. Phys.* **2007**, *127*, 084320.

[23] The $^2T_2$ state structure of $C_{10}H_{16}^+$ with T_d symmetry is a saddle point with a twofold degenerate imaginary wavenumber (i957 cm^{-1}).

[24] N. Polfer, B. G. Sartakov, J. Oomens, *Chem. Phys. Lett.* **2004**, *400*, 201.

[25] Possible candidates for the 3120 and 3177 cm^{-1} bands are combination and overtone transitions involving at least three quanta of σ_{CC} and/or β_{CH} modes. Other attractive candidates are combination bands of the intense σ_{CH} modes ν_6(e) and ν_7(a_1) with strongly IR-active low-wavenumber, skeletal, degenerate e modes at 300 and 554 cm^{-1} with $I = 255$ and 782 km mol^{-1}, respectively.

[26] P. A. Gunchenko, A. M. Makukhina, A. A. Novikovskii, A. G. Yurchenko, M. Serafin, P. R. Schreiner, A. A. Fokin, *Theor. Exp. Chem.* **2009**, *45*, 246.

[27] a) D. Roth, O. Dopfer, *Phys. Chem. Chem. Phys.* **2002**, *4*, 4855; b) N. Solcà, O. Dopfer, *J. Am. Chem. Soc.* **2004**, *126*, 9520; N. Solcà, O. Dopfer, *Chem. Phys. Lett.* **2000**, *325*, 354.

[28] IRPD spectra of $C_{10}H_{16}^+\cdot(N_2)_n$ show that the absorption of a single IR photon with 2600 cm^{-1} is sufficient to evaporate three but not four N_2 ligands, yielding an interval of 650–900 cm^{-1} (7.5–11 kJ mol^{-1}) for their average binding energy.

[29] a) O. Dopfer, *Int. Rev. Phys. Chem.* **2003**, *22*, 437; b) O. Dopfer, *Z. Phys. Chem.* **2005**, *219*, 125.

[30] The widths for L = He are smaller than for $L = N_2$ due to the smaller rotational temperature achieved for the more weakly bound He clusters.

